

Document made available under the Patent Cooperation Treaty (PCT)

International application number: PCT/US05/012173

International filing date: 09 April 2005 (09.04.2005)

Document type: Certified copy of priority document

Document details: Country/Office: US
Number: 60/561,164
Filing date: 10 April 2004 (10.04.2004)

Date of receipt at the International Bureau: 20 June 2005 (20.06.2005)

Remark: Priority document submitted or transmitted to the International Bureau in compliance with Rule 17.1(a) or (b)



World Intellectual Property Organization (WIPO) - Geneva, Switzerland
Organisation Mondiale de la Propriété Intellectuelle (OMPI) - Genève, Suisse

1331206



THE UNITED STATES OF AMERICA

TO ALL TO WHOM THESE PRESENTS SHALL COME:

UNITED STATES DEPARTMENT OF COMMERCE

United States Patent and Trademark Office

June 08, 2005

THIS IS TO CERTIFY THAT ANNEXED HERETO IS A TRUE COPY FROM THE RECORDS OF THE UNITED STATES PATENT AND TRADEMARK OFFICE OF THOSE PAPERS OF THE BELOW IDENTIFIED PATENT APPLICATION THAT MET THE REQUIREMENTS TO BE GRANTED A FILING DATE.

APPLICATION NUMBER: 60/561,164

FILING DATE: April 10, 2004

RELATED PCT APPLICATION NUMBER: PCT/US05/12173



Certified by

Under Secretary of Commerce
for Intellectual Property
and Director of the United States
Patent and Trademark Office

041004

14230 U.S. PTO

PTO/SB/16 (9/98)

Approved for use through 07/31/2006. OMB 0651-0042

U.S. Patent and Trademark Office; U.S. DEPARTMENT OF COMMERCE

Under the Paperwork Reduction Act of 1995, no persons are required to respond to a collection of information unless it displays a valid OMB control number.

PROVISIONAL APPLICATION FOR PATENT COVER SHEET

This is a request for filing a PROVISIONAL APPLICATION FOR PATENT under 37 CFR 1.53(c).

Express Mail Label No. ER 916165347 US

INVENTOR(S)					
Given Name (first and middle (if any))		Family Name or Surname		Residence (City and either State or Foreign Country)	
Michael Norman		Trainer		186 Fretz Road, Telford, PA 18969	
Additional inventors are being named on the <u>zero</u> separately numbered sheets attached hereto					
TITLE OF THE INVENTION (500 characters max)					
Particle size measuring systems using dynamic light scattering					
Direct all correspondence to: CORRESPONDENCE ADDRESS					
<input type="checkbox"/> Customer Number: 					
OR					
<input checked="" type="checkbox"/> Firm or Individual Name		Michael Trainer			
Address		186 Fretz Road			
Address					
City		Telford		State	PA
Country		USA		Telephone	2157238894
				Zip	18969
				Fax	
ENCLOSED APPLICATION PARTS (check all that apply)					
<input checked="" type="checkbox"/> Specification Number of Pages <u>27</u>		<input type="checkbox"/> CD(s), Number _____			
<input checked="" type="checkbox"/> Drawing(s) Number of Sheets <u>25</u>		<input type="checkbox"/> Other (specify) _____			
<input type="checkbox"/> Application Data Sheet. See 37 CFR 1.76					
METHOD OF PAYMENT OF FILING FEES FOR THIS PROVISIONAL APPLICATION FOR PATENT					
<input checked="" type="checkbox"/> Applicant claims small entity status. See 37 CFR 1.27.		FILING FEE Amount (\$)			
<input checked="" type="checkbox"/> A check or money order is enclosed to cover the filing fees.		<div style="border: 1px solid black; padding: 10px; width: fit-content; margin: 0 auto;">\$80.00</div>			
<input type="checkbox"/> The Director is hereby authorized to charge filing fees or credit any overpayment to Deposit Account Number: _____					
<input type="checkbox"/> Payment by credit card. Form PTO-2038 is attached.					
The invention was made by an agency of the United States Government or under a contract with an agency of the United States Government.					
<input checked="" type="checkbox"/> No.					
<input type="checkbox"/> Yes, the name of the U.S. Government agency and the Government contract number are: _____					

[Page 1 of 2]

Respectfully submitted,

SIGNATURE: Michael TrainerTYPED or PRINTED NAME Michael TrainerTELEPHONE 215 723 8894Date April 10, 2004REGISTRATION NO. _____
(if appropriate)

Docket Number: _____

USE ONLY FOR FILING A PROVISIONAL APPLICATION FOR PATENT

This collection of information is required by 37 CFR 1.51. The information is required to obtain or retain a benefit by the public which is to file (and by the USPTO to process) an application. Confidentiality is governed by 35 U.S.C. 122 and 37 CFR 1.14. This collection is estimated to take 8 hours to complete, including gathering, preparing, and submitting the completed application form to the USPTO. Time will vary depending upon the individual case. Any comments on the amount of time you require to complete this form and/or suggestions for reducing this burden, should be sent to the Chief Information Officer, U.S. Patent and Trademark Office, U.S. Department of Commerce; P.O. Box 1450, Alexandria, VA 22313-1450. DO NOT SEND FEES OR COMPLETED FORMS TO THIS ADDRESS. SEND TO: Mail Stop Provisional Application, Commissioner for Patents, P.O. Box 1450, Alexandria, VA 22313-1450.

If you need assistance in completing the form, call 1-800-PTO-9199 and select option 2.

22154 U.S. PTO

601561164

041004

Please confirm that a prior provisional patent application ("Methods and Apparatus for Determining the Size and Shape of Particles") was received and filed. These documents were sent by express mail on March 6, 2004. The express mail tracking number was ER 493082116 US. Please include a note, with your answer, in the enclosed self addressed envelope, which was included for confirmation of this new application enclosed.

Thank you,

Michael Trainer

Particle size measuring systems using dynamic light scattering

Inventor: Michael Trainer

1

Particle size measuring systems using dynamic light scattering

Inventor: Michael Trainer

Dynamic light scattering has been used to measure particle size by sensing the Brownian motion of particles. Since the Brownian motion velocities are higher for smaller particles, the Doppler broadening of the scattered light is size dependent. Both heterodyne and homodyne methods have been employed to create interference between light scattered from each particle and either the incident light beam (heterodyne) or light scattered from the other particles (homodyne) of the particle ensemble. Heterodyne detection provides much higher signal to noise due to the mixing of the scattered light with the high intensity light from the source which illuminates the particles. This disclosure describes concepts which use a beamsplitter and a mirror or partial reflector to mix the light from the source with light scattered by the particles. This disclosure also describes concepts which use a fiber optic coupler to mix the light from the source with light scattered by the particles.

In Figure 1 a light source is focused through a pinhole by lens 1 to remove spatial defects in the source beam. The focused beam is recollimated by lens 2 which projects the beam through an appropriate beamsplitter (plate, cube, etc.). The diverging light source, lens 1, pinhole 1, and lens 2 could all be replaced by an approximately collimated beam, as produced by certain lasers. This nearly collimated beam is focused by lens 3 into the particle dispersion which is contained in a sample cell or container with a window to pass the beam. The focused beam illuminates particles in the dispersion and light scattered by the particles passes back through the window and lens 3 to be reflected by the beamsplitter through lens 4 and pinhole 2 to a detector. A portion of the incident collimated source beam is reflected from the beamsplitter towards a mirror, which reflects the source light back through the beamsplitter and through the same lens 4 and pinhole 2 to be mixed with the scattered light on the detector. This source light provides the local oscillator for heterodyne detection of the scattered light from the particles. The mirror position must be adjusted to match (to within the coherence length of the source) the optical pathlengths traveled by the source light and the scattered light. This is accomplished by approximately matching the optical path length from the beam splitter to the scattering particles and from the beam splitter to the mirror. The interference between scattered and source light indicates the velocity and size of the particles. The visibility of this interference is maintained by pinhole 2 which improves the spatial coherence on the detector. Pinhole 2 and the aperture of lens 3 restrict the range of scattering angle (the angle between the incident beam and the scattered light direction) to an angular range around 180 degrees. Multiple scattering can be reduced by moving the focus of lens 3 to be close to the inner surface (the interface of the dispersion and the window) of the sample cell window. Then each scattered ray will encounter very few other particles before reaching the inner window surface. Particles far from the window will show multiple scattering, but they will contribute less to the scattered light because pinhole 2 restricts the acceptance aperture. The sample cell could be a removable cuvette. Multiple scattering is reduced as long as the short distance of inner window surface to the

focal point (in the dispersion) of lens 3 is maintained by appropriate position registration of the cuvette.

This design can provide very high numerical aperture at the sample cell, which improves signal to noise, reduces multiple scattering, and reduces Mie resonances in the scattering function. Light polarization is also preserved, maximizing the interference visibility.

Figure 2 shows another version of this concept where lower scattering angles are measured by separating the incident and scattered beams. Mie resonances are improved at lower scattering angles. Also multiple scattering is reduced by eliminating the scattering contribution of particles far from the lens 3 focus. Only particles in the volume of the intersection of the incident and scattered light cones contribute to scattering passing through pinhole 2. If this volume is close to the inner wall of the sample cell window, all scattered rays will have a very short transit through the particle dispersion. The sample cell window should be tilted slightly so that the Fresnel reflection of the incident beam from the window surface does not enter pinhole 2 though the aperture on lens 4. However if this reflection were large enough, the window surface reflected light could provide the local oscillator without the need for the mirror by providing the proper window tilt to pass the reflection through the lens 3 aperture and pinhole 2.

Figure 3 shows a similar configuration to Figures 1 and 2, except that the mirror has been replaced by a retro-reflector or corner cube. The alignment of this configuration will be more stable because the retro-reflector reflects light at 180 degrees to the incident beam over a wide range of incident angles.

Figure 4 shows a configuration where the local oscillator is created by a reflection from the coated convex surface of a plano-convex lens (lens 5) or some other partially reflecting convex surface. The center of curvature of this convex surface coincides with the focus of the incident laser beam, without lens 3, in air. This convex surface provides a partially reflecting surface which is normal to the incident rays. Therefore, the reflected light will focus through pinhole 2 along with the scattered light even though the scattering surface is not coincident with the focus. If the beam focus were focused at the inner surface of the sample cell window, then this planar window surface could provide the reflection for the local oscillator, without the need for the convex surface. However, then the signal would be sensitive to the motion of the sample cell, requiring stable mechanical registration of the cuvette. Lens 5 can be attached firmly to the structure of the optical system, maintaining the high mechanical stability required by an interferometer. Also the reflectivity of the convex surface is more easily increased by reflective coatings, than the inner surface of the sample cell window. Lens 5 could also be replaced by a plano partially reflecting mirror between the beamsplitter and lens 3. The tilt of this partially reflecting mirror must be adjusted to reflect a portion of source light back through lens 4 and pinhole 2. These configurations could also be used with a fiber optic coupler instead of a beam splitter, with appropriate coupling optics at each port of the coupler.

In some cases, the beam focus will define an interaction volume, in the dispersion, which is too small to contain a statistically significant number of particles. The interaction volume is the volume of the particle dispersion which contributes to the scattered light collected by the optics. In particular, a sample of larger particles at low concentration may not be representative of the total sample if the exchange of particles in and out of interaction volume is slow. In this case a larger interaction volume is required to maintain sufficient particles in the beam. So changing the beam focus size and divergence may be appropriate in some applications. Figures 5 and 6 show the interchange of two lenses, lens 3A and lens 3B, to change the size of the interaction volume in the dispersion. In each case the focus of lens 3A or 3B is placed in the dispersion, with a position which can be adjusted by moving this lens in any direction. For any position of the lens, the scattered light will pass back through pinhole 2 with the local oscillator reflection from the mirror. The partial reflecting mirror in Figures 5 and 6 could also be replaced by the plano partial reflecting mirror between the beamsplitter and lens 3A or lens 3B, as described previously for Figure 4.

Another aspect of Figures 5 and 6 is the use of a partially reflecting mirror to produce the local oscillator for heterodyne detection and to monitor the laser intensity fluctuations. The source light which passes through the partially reflecting mirror is focused by lens 5 onto detector 2. The signal from detector 2 is used to correct the signal on detector 1 for intensity variations and noise in the light source as described by the inventor in this disclosure and another disclosure. The mirror could also be removed to measure the homodyne (self beating) spectrum of the scattered light from the particles.

Also notice that lens 1 and pinhole 1 have been removed in Figures 5 and 6 to show the configuration without removal of spatial defects in the beam. For example, the source could be a laser diode in these figures. If a low divergence beam from a collimated laser, such as a gas laser, were used, the collimating lens 2 could also be eliminated.

Figure 7 shows a probe version of this invention which can be dipped into the dispersion in a container such as a beaker. Since the particles may settle, the beam is folded by a mirror just before passing through the window. Then the beam is projected into the sample in a direction nearly perpendicular to the direction of gravitational settling so that as particles settle out of the interaction volume, they are replaced by other particles which settle into the volume from above. As shown before, the partially reflecting mirror could be fully reflecting. This mirror could also be eliminated for homodyne detection or replaced by a partially reflecting convex surface placed between lens 3 and the window.

Figure 8 shows another variation where a partially reflecting flat mirror, which produces the local oscillator, is placed in the collimated portion of the beam between the beamsplitter and lens 3. The tilt of this mirror would be adjusted to send the reflection back through pinhole 2. The partially reflecting local oscillator mirror can be placed in this position (between the beamsplitter and the next optic towards the particle sample) in all configurations in this disclosure, where the light is nearly collimated through the beamsplitter.

Another issue is the shift in the heterodyne spectrum due to convection currents in the sample. This is usually small when the divergence of the beam focus is low and the focus is close to the interface between the dispersion and the window. However, this problem may be reduced by surrounding the interaction volume with a chamber as shown in Figure 9. This chamber may be made out of material with high thermal capacity and conductivity to bring the interaction volume to thermal equilibrium. Also the height of the inner chamber wall must be sufficient distance from the interaction volume to prevent the larger particles from settling out of the interaction volume during data collection.

All of these configurations can generate a local oscillator for heterodyne detection using the following methods. In all cases the reflector, which generates the local oscillator, must be held in a stable location relative to the rest of the interferometer:

- 1) partially or totally reflecting mirror at the beam splitter, as shown in Figure 1 and Figure 5
- 2) flat partially reflecting surface close to the focus of the beam in the sample. If this is the inner surface of a removable cuvette, it must have stable mechanical registration to avoid interferometric noise due to motion of the partially reflective surface. This would replace the mirror in item 1.
- 3) A flat partially reflecting flat surface between the beamsplitter and lens 3 could replace the mirror in item 1
- 4) A partially reflective convex surface with center of curvature at the beam focus in air could replace the mirror in item 1.

One of the key advantages of this invention is that the beam focus in the dispersion does not need to be coincident or near to a partially reflecting surface, such as the inner surface of a cuvette. If the inner surface of cuvette is not close to the beam focus in the dispersion, very little of the reflection from that surface will be returned through pinhole 2 to contribute interferometric noise from small motion of the surface. This allows the use of inexpensive cuvettes whose poor tolerances may not accommodate the requirements of the optical interferometry in the systems shown above.

Another advantage of these designs is the ease of alignment. All of the components in each design can be positioned to within standard machining tolerances. Only two components need alignment during manufacture: the pinhole and/or the local oscillator reflector. These systems have the following advantages over fiber optic systems:

- better interferometric efficiency in both polarization and coherence
- more flexibility for choice of scattering angle
- better photometric efficiency
- better control over the local oscillator level
- higher numerical aperture in the scattering volume
- simple adjustment of scattering volume numerical aperture and position in the sample
- adjustable scattering volume
- lower multiple scattering
- lower cost

In the cases where fiber optic systems may have other advantages (such as electromagnetic immunity) their designs can be changed to gain some of the advantages which are listed above. The following describes some concepts for fiber optic systems.

Fiber optic methods and apparatus

The basic fiber optic interferometer is illustrated in Figure 10. A light source is focused into port 1 of a fiber optic coupler. This source light is transferred to port 4 and light scattering optics which focus the light into the particle dispersion and collect light scattered from the particles. This scattered light is transferred back through the fiber optic and coupler to the detector on port 2. If the coupler has a third port, a portion of the source light also continues on to port 3 which may provide a local oscillator with a reflective layer. If the local oscillator is not provided at port 3, a beam dump or anti-reflective layer may be placed onto port 3 to eliminate the reflection which may produce interferometric noise in the fiber optic interferometer. The beam dump could consist of a thick window which is attached to the tip of the fiber with transparent adhesive whose refractive index nearly matches that of the fiber and the window. This will reduce the amount of light which is Fresnel reflected back into the fiber at the fiber tip. The other surface of the window can be anti-reflection coated, and/or be sufficiently far (thick window) from the fiber tip, so that no light, which is reflected from that surface, can enter the fiber.

Figure 11 shows one version of the scatter optics on port 4. A lens or gradient index optic (GRIN) focuses the source light into the particle dispersion in a cuvette through a transparent wall of the cuvette. A partially-reflective layer on the tip of the fiber or on the surface of the GRIN rod, at the fiber/GRIN gap, provides the local oscillator light to travel back through port 4 with light scattered by the particles. If the fiber surface is partially reflecting, the GRIN surface could be anti-reflection coated or it could be placed sufficiently far from the fiber to avoid reflections from the GRIN surface back into the fiber. Reflections from both surfaces could produce an optical interferometric signal which may contaminate the heterodyning signal from the scattering particles. The reflected source light and the scattered light, from particles in the cuvette, travel back through the coupler and are combined on the detector at port 2. The interference between these two light components is indicative of the Brownian motion of the particles and the particle size. Since the local oscillator is generated at the exit surface of port 3 or port 4, as opposed to the cuvette surface, the interference signal is not degraded by small errors in the position of the cuvette surfaces, allowing use of inexpensive disposable cuvettes. The local oscillator is provided by light reflected from either port 3 or port 4 fiber optic. The reflection is provided by a partially reflective surface close to exit surface of the fiber or a layer on the fiber itself as shown in Figures 14 and 13, respectively. Both of these methods can be used on either port 3 or port 4 to create a reflection for the local oscillator. Since the partially reflecting surface is at the exit of the fiber optic, no optical alignment is required for the scattered light or the local oscillator light.

Figure 11B shows another concept where the reflective layer is placed on the end of GRIN rod 1, which is coated to provide the local oscillator reflection. The GRIN rod pitch is chosen so that this surface is conjugate to the fiber tip. Spacing, anti-reflection coating or index matching can be used in the fiber/GRIN gap to reduce reflection at that surface. This configuration has the advantage that only GRIN rod 1 needs to be coated. So hundreds of GRIN rods could be coated in one evaporation or sputtering operation. GRIN rod 2 then transfers the beam into the cuvette. Conventional lenses could also be used to accomplish this design by replacing each GRIN rod with a lens and placing a planar reflecting surface at the intermediate plane which is conjugate to the fiber tip.

Figure 11B also shows a conventional lens version of this idea which uses a coated window surface at the intermediate conjugate plane to create the local oscillator reflection.

Placing a reflective layer on the tip of the fiber could require placing the entire fiber optic coupler into a vacuum chamber for evaporated or sputtered coatings. The design shown in Figure 12 shows a fiber tip assembly which is removable from the coupler port. This design allows many fiber tip assemblies to be placed into the sputtering chamber at one time to reduce coating costs. Only the assembly of male fiber optic connectors #2 and #3, or connector #3 alone, need to be placed into the vacuum chamber for sputtering a partially reflective layer on the tip of connector #3. Index matching gel is placed in the gap between connectors #1 and #2 to reduce reflected light at these surfaces. The GRIN rod assembly with attached female connector can be removed and replaced with other assemblies containing different types of lenses to change the interaction volume (the volume of the particle dispersion which contributes to the scattered light collected by the optics) in the particle dispersion to control the number of particles viewed by the optics. This can be important when concentrations are low and only a few particles are in the interaction volume, producing poor signal statistics. The GRIN rod could also be replaced by a conventional lens. In either case, the lens focal length and position can be adjusted to change the interaction volume, scattering angle range, and numerical aperture (to control scattering sample depth and multiple scattering).

The male/male connector assembly is easily manufactured by butting two male connectors, back-to-back, through a sleeve and pushing a fiber through the entire assembly. This fiber is potted and end polished in both connectors using standard techniques.

Other types of optical systems could also be attached to this port. An example of a probe attachment for insertion directly into the dispersion is shown in Figure 15. The female connector is part of the probe assembly (Figure 15) and the standard GRIN assembly (Figure 12); so that both of these assemblies can be interchanged onto the same coupler without any optical alignment. The source light exits the probe and enters the particle dispersion approximately perpendicular to gravity so that particles that settle out of the interaction volume are replaced by other particles which settle into the volume from above. In all of these cases, the coupling system which consists of male connectors #2 and #3 can be eliminated if the local oscillator is placed directly onto either the fiber tip

at port 3 or the fiber tip of male connector #1. And in both of these assembly designs, the partially reflecting surface, for producing the local oscillator, can be placed on any surface which is conjugate to the exit tip of the port 4 fiber optic and which is mechanically stable with respect to the port 4 tip. One example of this is a flat partial reflector between lenses 2 and 3 in Figure 15, or adding a second lens in Figure 12 to create an intermediate plane, which is conjugate to the fiber tip, where the partially reflecting surface is placed. However, some optical alignment may be required in these designs.

Another attachment design could use all anti-reflection coated optics, without the partially reflecting surfaces, to completely eliminate any local oscillator source, for homodyne detection.

Also note that in all of the heterodyne designs with the local oscillator reflector in the scatter sensing arm, the optical path difference between the scatter light path and the local oscillator path (the difference between the optical path length from the local oscillator partial reflector to the detector and the scattering particle to the detector) must be less than the coherence length of the light source to provide sufficient interferometric visibility.

For both the fiber optic and non-fiber optic systems, the local oscillator reflection can be generated at certain surfaces. All other surfaces may be tilted and/or anti-reflection coated so as to contribute minimal interferometric signal on the detector. In both the fiber and non-fiber systems, the source beam is focused within the cuvette (or sample cell). If the focused point is far into in the dispersion (see Figure 16), the local oscillator reflection must be created at another surface as described above. In any case, a spring could be employed to press the cuvette against a registration surface, as shown in Figure 16, to firmly register and position the cuvette. The spring could also be replaced by a clamping screw to avoid the low frequency mechanical resonances of the spring. The cuvette (and cuvette holder) must be mechanically registered to the optical system for two reasons. If the cuvette surface reflection generates the local oscillator, movement of the surface will create interferometric noise. Also if the cuvette and/or the particles move relative to the optics due to mechanical vibration, non-Brownian Doppler shifts of the scattered light will be detected which will confound the size determination.

This positional registration is even more critical when the beam focus is at the inner surface of the cuvette (the surface contacting the dispersion) and the reflection from that surface is used to generate the local oscillator (see Figure 17). Then any motion of the cuvette will create interferometric noise in the heterodyne signal. So the cuvette must be pinned against a reference surface as shown in Figure 17, where a spring holds the cuvette against an inner surface of the cuvette holder. The beam focus might be placed close to this inner surface to either provide the local oscillator from that surface or to reduce multiple scattering into the pinhole or fiber optic. If the only reason is to reduce multiple scattering and the local oscillator reflection is produced at another surface, then the incident light beam might approach the cuvette at a non-normal incidence angle (see Figure 18 which is the top view of Figure 17) so that the reflected light from that inner

surface cannot pass back through the optical system and through the pinhole or fiber to the detector. All reflected light, except for the local oscillator reflection, should be suppressed to reduce interferometric noise from mechanical vibrations and from laser phase noise and to reduce reflections back into a laser source to reduce laser noise.

For small particles, the heterodyne signals will be buried in laser source noise. Figure 5, Figure 6, and Figure 7 show detector 1, which measures the heterodyne signal from the particles. In Figure 19, detector 2 is the heterodyne detector. Figure 5, Figure 6, and Figure 7 show an additional detector 2, which measures the intensity of the local oscillator laser noise. Figure 19 also shows additional detectors, detector 1 (the rear facet detector on the laser) and detector 3 (a laser power monitor on port 3 of the fiber coupler). Any of these additional detectors, or any detector which monitors the laser power, can be used to monitor the laser noise. Another possibility is to monitor the light that has passed through the particle dispersion by placing a detector in the sample cell. In any event, if we define a heterodyne detector current as I_1 and the laser monitor detector current as I_2 we obtain the following equations which hold for each of the heterodyne detectors.

$$I_1 = \sqrt{R \cdot I_o(t) \cdot I_s(t)} \cdot \cos(F \cdot t + A) + R \cdot I_o$$

$$I_1 = \sqrt{R \cdot I_o(t) \cdot S(1-R) I_o} \cdot \cos(F \cdot t + A) + R \cdot I_o$$

$$I_2 = K \cdot I_o(t)$$

where:

$\cos(x)$ = cosine of x

K is a constant which includes reflectivity of the beamsplitter

R is the reflectivity of the beamsplitter

\sqrt{x} = square root of x

$I_o(t)$ is the source beam intensity as function of time t

F is the heterodyne beat frequency at a heterodyne detector due to the motion of the scatterer which produces $I_s(t)$. And A is an arbitrary phase angle for the particular particle.

$I_s(t)$ is the scattered light intensity from the particle:

$I_s(t) = S \cdot (1-R) \cdot I_o(t)$ where S is the scattering efficiency or scattering crosssection for the particle

The light source intensity will consist of a constant portion I_{oc} and noise $n(t)$:

$$I_o(t) = I_{oc} + n(t)$$

We may then rewrite equations for I1 and I2:

$$I1 = \sqrt{S*(1-R)*R}*(I_{oc} + n(t))*\cos(F*t + A) + R*(I_{oc} + n(t))$$

$$I2 = K*(I_{oc} + n(t))$$

If we use high pass filters to only accept only the higher frequencies, which contain the size information, we obtain high pass signals for I1 and I2:

$$I1_{hp} = \sqrt{S*(1-R)*R}*I_{oc}\cos(F*t + A) + R*n(t)$$

$$I2_{hp} = K*n(t)$$

Where we have assumed that $n(t)$ is much smaller than I_{oc} . And also $n(t)$ is the portion of the laser noise that is passed by the high pass filter bandwidth (see below). In certain situations, these high pass filters are replaced by band pass filters which only pass frequencies carrying particle information.

The laser noise can be removed to produce the pure heterodyne signal, I_{diff} , through the following relationship:

$$I_{diff} = I1_{hp} - (R/K)*I2_{hp} = \sqrt{R*(1-R)*S}*I_{oc}\cos(F*t + A)$$

This relationship is realized by high pass filtering of each of the I1 and I2 detector currents. One or both of these filtered signals are amplified by programmable amplifiers, whose gains and phase shifts are adjustable. The difference of the two outputs of these amplifiers is generated by a difference circuit or differential amplifier. With no particles in the beam, the gain and phase shift of at least one of the programmable amplifiers is adjusted, under computer or manual control, to minimize the output of the difference circuit (i.e. $(\text{gain } I2)*R/K = 1$). At this gain, the source intensity noise component in the heterodyne detector beat signal, with particles present, is removed in the difference signal, which is fed to an analog to digital converter (A/D), for inversion to particle size.

This entire correction could be accomplished in the computer by using a separate A/D for each filtered signal and doing the difference by digital computation inside the computer. The phase and gain adjustments mentioned above, without particles in the beam, could be accomplished digitally. Then the coefficient ratio R/K can be calculated to be used in the equation for I_{diff} , using the following equation:

$$R/K = I1_{dc}/I2_{dc}$$

Where $I1_{dc}$ and $I2_{dc}$ are the DC offsets of the unfiltered signals I1 and I2, respectively.

If both signals were digitized separately, other correlation techniques could be used to reduce the effects of source intensity noise. In any case, the beamsplitter reflection is adjusted to obtain shot noise limited heterodyne detection, with excess laser noise removed by the difference circuit or difference calculation shown above.

These noise correction techniques can be applied to any heterodyning system by simply adjusting the filtering of currents I1 and I2 to pass the signal of interest, while blocking the low frequency component (Ioc) of I_o(t). Excess laser noise and other noise components, which are present in both the heterodyne signal and the light source, can be removed from the signal of interest through this procedure. One excellent application is correction of signals in Doppler velocimetry, as described by this inventor in other disclosures. Another application is dynamic light scattering, where the heterodyne signal is contaminated by laser source noise in the optical mixing process. The filters on I1 and I2 would be designed to pass the important portion of the Doppler broadened spectrum and to remove the large signal offset due to the local oscillator. Then by using the subtraction equation for Idiff described on page 10 the effects of laser noise can be removed from the Doppler spectrum, improving the particle size accuracy. In the case of fiber optic heterodyning systems, the laser monitor current, I2, could be obtained at the exit of the unused output port (port 3 in Figure 19) of the fiber optic coupler which is used to transport the light to and from the particle sample, because this port carries light only from the optical source, without any scattered light. I2 could also be obtained from the laser detector (for example the rear facet detector on a laser diode as shown by detector 1 in Figure 19). This subtraction shown in the equation on page 10 for Idiff could be accomplished by the analog difference circuit or by digital subtraction after digitization of both the filtered contaminated signal and the filtered source monitor as outlined on page 9 and 10. This procedure could also be accomplished using the unfiltered signals, but with much poorer accuracy due to the large signal offsets.

Using Figure 19 we can describe another version of this correction which simply measures the power spectrum at port 2 (detector 2) and port 3 (detector 3) in Figure 19. The signal at port 1 (detector 1) could also be used in place of the detector 3 signal. Let us define the following measurements:

P2bkg = power spectrum measured at port 2 with clean dispersant (without particles) in the sample region

P3bkg = power spectrum measured at port 3, while P2bkg is being measured on port 2

P2meas = power spectrum measured at port 2 from the particle dispersion (with particles) in the sample region

P3meas = power spectrum measured at port 3, while P2meas is being measured on port 2

I3dc = DC offset or constant portion of signal producing P3meas

I2dc = DC offset or constant portion of signal producing P2meas

Then the measured power spectrum, P_{2meas} , can be corrected for the background power spectrum and the drift in the background power spectrum by using the following equations, where $P(f=0)$ is the power spectral density at frequencies close and equal to zero:

$$P_{corrected} = P_{2meas} - P_{2bkg} - ((I_{2dc}/I_{3dc})^2) * (P_{3meas} - P_{3bkg})$$

or

$$P_{corrected} = P_{2meas} - P_{2bkg} - (P_{2meas}(f=0)/P_{3meas}(f=0)) * (P_{3meas} - P_{3bkg})$$

The background corrected power spectrum, $P_{corrected}$, would then be inverted to obtain the particle size distribution.

The correction described for Idiff on page 10 removes common mode noise between the scattered heterodyne signal and the laser monitor. This correction is made directly to the signal. While this technique is useful in the case of dynamic light scattering and many other heterodyne systems, another method may be more easily implemented to correct the power spectrum in dynamic light scattering, for the noise component due to laser noise. In most cases the local oscillator is adjusted to provide shot noise limited detection. However, usually some excess laser noise (called laser noise in the following description), beyond the shot noise, is observed. We will start with some definitions for power spectral densities which are all functions of frequency f :

P_{sd} = total power spectral density of the scattering detector (detector 1 for Figures 5, 6, and 7 and detector 2 for Figure 19)

P_{sc} = power spectral density component of the scattering detector current due to particle scattering

P_{ssh} = shot noise component of power spectral density of the scattering detector

P_{sls} = laser noise component of power spectral density of the scattering detector

P_{ld} = total power spectral density of the laser monitor detector (detector 2 for Figures 5, 6, and 7 and detector 1 or 3 for Figure 19)

P_{lsh} = shot noise component of power spectral density of the laser monitor detector

P_{lls} = laser noise component of power spectral density of the laser monitor detector

I_{os} = mean detector current of the scattering detector

I_{ol} = mean detector current of the laser monitor detector

$$P_{ssh} = 2 \cdot e \cdot (I_{os}) \quad (\text{scatter detector shot noise})$$

$$P_{lsh} = 2 \cdot e \cdot (I_{ol}) \quad (\text{laser monitor detector shot noise})$$

Where e is the electron charge

$$P_{sls} = B \cdot g(f, i_c) \cdot (I_{os})^2 \quad (\text{scatter detector laser noise component})$$

$$P_{lls} = B \cdot g(f, i_c) \cdot (I_{ol})^2 \quad (\text{laser monitor detector laser noise component})$$

Since these noise sources and scattering signals are uncorrelated, the following equations hold:

$$P_{sd} = P_{sc} + P_{ssh} + P_{sls}$$

$$P_{ld} = P_{lsh} + P_{lls}$$

$$P_{sd} = (P_{sc} + 2 \cdot e \cdot (I_{os}) + B \cdot g(f, i_c) \cdot (I_{os})^2) \cdot G_s(f)$$

$$P_{ld} = (2 \cdot e \cdot (I_{ol}) + B \cdot g(f, i_c) \cdot (I_{ol})^2) \cdot G_l(f)$$

Where B is a constant and $g(f, i_c)$ is the spectral function for laser noise, f is frequency and i_c is laser current. $G_s(f)$ and $G_l(f)$ are the electronic spectral gain of the detector electronics for the scatter detector and laser monitor detector, respectively.

From these last two equations, we want to determine P_{sc} , the power spectrum component due to the light scattered from the particles. Solving these two equations for P_{sc} , we obtain:

$$P_{sc}(f) = (P_{sd}(f)/G_s(f)) - (2 \cdot e \cdot (I_{os})) - (((P_{ld}(f)/G_l(f)) - (2 \cdot e \cdot (I_{ol}))) \cdot (I_{os})^2 / (I_{ol})^2)$$

This equation assumes that the excess laser induced amplitude noise (noise in excess of the shot noise) is proportional to the mean detector current due to the laser. This assumption is described by the proportionality to the square of the mean detector currents of power spectral density in the following equations:

$$P_{sls} = B \cdot g(f, i) \cdot (I_{os})^2 \quad (\text{scatter detector laser noise component})$$

$$P_{lls} = B \cdot g(f, i) \cdot (I_{ol})^2 \quad (\text{laser monitor detector laser noise component})$$

However, in general the excess noise components may have a more complicated and unknown dependence given by the function gn :

$P_{sls} = B * g_n(f, i, I_{os})$ (scatter detector laser noise component)

$P_{lls} = B * g_n(f, i, I_{ol})$ (laser monitor detector laser noise component)

In this case, the functional dependence $g_n(f, i, I)$ could be determined by measuring P_{sls} and P_{lls} at various levels of I_{os} and I_{ol} . Since the function $g_n(f, i, I)$ could possibly change between lasers, an easier method is to adjust the mean detector currents, I_{os} and I_{ol} , to be equal with a variable optical attenuator, such as two polarizers with adjustable rotation angles. This attenuator could be placed on front of either the heterodyne detector or the laser monitor detector (as shown by detector 3 in Figure 19 for example). When I_{os} and I_{ol} are made equal, we obtain:

$$P_{sc} = (P_{sd}/G_s(f)) - ((P_{ld}/G_l(f)))$$

Another method is to measure P_{sd} and P_{ld} without any particles in the beam and calculate the ratio RT as a function of frequency:

$RT(f) = P_{sd}(f)/P_{ld}(f)$ without particles in the sample volume

Then $P_{sc}(f) = P_{sd}(f) - (RT(f) * P_{ld}(f))$ for particles in the sample volume

This is only an estimate to the true correction, but it may work well in cases where the excess noise and mean detector currents are not changing much.

Notice: any products, divisions, additions, or subtractions in this document between functions (or vectors) are assumed to be inner operations (i.e. the function(x) values at each value of x are multiplied, divided, added, or subtracted).

The noise correction can also be determined from background measurements and assumptions for the form of the power spectral density for the particles and for the noise. The power spectrum of the scatter detector current from particles under Brownian motion takes the form:

$$P(f) = 4 * I_o * I_s * (K/\pi) / (f^2 + K^2) \quad \text{for particles of a single size}$$

Where

x^2 is the square of quantity x

π is constant pi

$P(f)$ is the power spectral density of the detector current

f is the frequency of the detector current

Inventor: Michael Trainer

I_o is the detector current due to the local oscillator intensity

I_s is the detector current due to the mean scattered light intensity

K is a constant which is particle size dependent

The total power spectral density measured from a group of particles is given by:

$$P_t(f) = \sum_j (4 * I_o * I_{sj} * (K_j / \pi) / (f^2 + K_j^2)) + P_b(f)$$

Where the \sum_j is over each j th particle with scattering I_{sj} and constant K_j .

$P_b(f)$ is the power spectral density of the detector current due to background such as excess laser noise and shot noise. $P_b(f)$ is usually measured on clean dispersant without particles. Examination of these equations provides the following approximations:

$$P_t(\infty) = P_b(f)$$

$P_b(\infty) = B$ at high frequencies, the background spectrum is white

The spectral density $P_b = \text{constant}$ at high frequencies

$$P_t(\sim\infty) = A / (f^2 + C) + B \text{ because at high frequencies } f \gg K_j$$

This dependence is illustrated in Figure 24, which shows the measurement of $P_t(f)$ in three different frequency bands. This can be accomplished by integration of the digitally generated power spectral density over these frequency bands or by using analog electronic filters and RMS modules to measure the power in the bands. These bands must be chosen at frequencies where the approximations, which are shown above, hold. The analog filters have an advantage, over digitally generated power spectrum measurements, that they can be placed at very high frequencies without affecting the design of the analog to digital converter and FFT algorithm used to measure the lower frequency power spectrum of the scatter signal from the particles. Then we can solve for B by using the following simultaneous equations to solve for A , B , and C :

$$P_t(f_1) = A / (f_1^2 + C) + B$$

$$P_t(f_2) = A / (f_2^2 + C) + B$$

$$P_t(f_3) = A / (f_3^2 + C) + B$$

Where $P_t(f_1)$ is the mean power spectral density in the band about frequency f_1 , and likewise for f_2 and f_3 .

If the frequency bands are at very high frequencies then f^2 is much greater than C and the following two simultaneous equations can be used:

$$P_t(f_1) = A/(f_1^2) + B$$

$$P_t(f_2) = A/(f_2^2) + B$$

And B is then given by:

$$B = (P(f_1) \cdot f_1^2 - P(f_2) \cdot f_2^2) / (f_1^2 - f_2^2)$$

Usually B is not a stable value and can change between successive digitized data sets and their corresponding power spectral density calculations. However, this calculation will determine the specific value of B for each calculation of $P_t(f)$ for each digital data set from the detector current.

$P_b(f)$ can be calculated from the value of B by using the following procedure. Measure $P_b(f)$ and B from the background signal of clean dispersant without particles. In this case B is simply the value of $P_b(f)$ at a very high frequency where $P_b(f)$ has a white noise spectrum. Let $B_0 = B$ and $P_{b0}(f) = P_b(f)$ from this clean dispersant measurement. Then when $P_t(f)$ and B are measured from a particle dispersion by the method described previously, $P_b(f)$ can be determined by:

$$P_b(f) = P_{b0}(f) - B_0 + B$$

$P_b(f)$ can also be calculated from a function of B or by using a lookup table, either which can be produced by many measurements of $P_b(f)$ for various values of B, by simply monitoring the instrument for a few days under different starting and environmental conditions. For example $P_b(f)$ could be fit to a polynomial, in f, whose coefficients are functions of B:

$$P_b(f) = B + G_1(B) \cdot f + G_2(B) \cdot f^2 + G_3(B) \cdot f^3 + \dots$$

And then the power spectrum of the signal component due to particle scattering is given by:

$$P_p(f) = P_t(f) - P_b(f)$$

This power spectral density $P_p(f)$ can then be inverted to produce the particle size distribution or it can be integrated on a logarithmic scale for deconvolution. This process can also be used directly with the logarithmic scale power spectral data. On the logarithmic frequency scale the following variable transformations are made:

$$x = \ln(f) \quad (\ln \text{ is the natural logarithm})$$

$$f = \exp(x)$$

Then creating the power spectrum on the logarithmic scale, $R(x)$ we obtain:

$$R(x) = P_t(f) \cdot \partial f / \partial x = f \cdot P_t(f) = P_l(x) = A / (\exp(x) + C \exp(-x)) + B \cdot \exp(x)$$

We can now measure the power in three logarithmic frequency bands, analogous to f1, f2 and f3 in the previous description. For example the three simultaneous equations now become:

$$R(x_1) = A/(\exp(x_1) + C\exp(-x_1)) + B*\exp(x_1)$$

$$R(x_2) = A/(\exp(x_2) + C\exp(-x_1)) + B*\exp(x_2)$$

$$R(x_3) = A/(\exp(x_3) + C\exp(-x_3)) + B*\exp(x_3)$$

Where $R(x)$ is the spectral power in the logarithmic frequency band at logarithmic frequency $x = \ln(f)$. And A , B , and C are new constants to be determined from solution of the simultaneous equations and $B*\exp(x)$ is the white noise background to be subtracted from the power spectrum measured in analogy to the linear frequency case described above. $R_b(x)$ can be calculated from the value of B by using the following procedure. Measure $R_b(f)$ and $B*\exp(x)$ from the background signal of clean dispersant without particles. In this case $B*\exp(x)$ is simply $R_b(x)$ at a very high frequency where $P_b(f)$ has a white noise spectrum. Let $B_0 = B$ and $R_{b0}(x) = R_b(x)$ from this clean dispersant measurement. Then when $R_t(x)$ and B are measured from a particle dispersion by the method described previously and the simultaneous equations are solved for B , $R_b(x)$ can be determined by:

$$R_b(x) = R_{b0}(x) - B_0*\exp(x) + B*\exp(x)$$

$$R_p(x) = R_t(x) - R_b(x)$$

$R_p(x)$ is the portion of the power spectrum on the logarithmic frequency scale, which is due to particle scatter. $R_p(x)$ is deconvolved by known methods to produce the particle size distribution.

In all of the power spectrum methods described above, all of the digitized signal samples collected from the particle dispersion consist of a group of data sets, which are collected sequentially. Each data set consists of a group of sequential digitized samples of the signal. In all of the cases described above, the power spectrum for each data set is corrected by calculations using measurements made during that set of digitized signal samples. The change of the power spectrum background should not be significant during any one data set, so that the power spectrum from each data set is corrected using the most accurate correction parameters present during the period of that data set. All of these corrected power spectra are then added together to obtain the final corrected power spectrum. This could also be accomplished by adding up all of the uncorrected power spectra and all of the corrections (corrected background to subtract from the measured power spectrum), and then subtract the sum of corrected backgrounds from the sum of measured power spectra to obtain the final corrected power spectra. The only requirement is that the corrections must be calculated at sufficiently short intervals such that the background characteristics can be accurately described by one set of parameters during any single data set, even though the background may be changing significantly during the entire data collection period.

Another improvement to signal to noise can be gained by analog filtering of the scatter signal before signal digitization and calculation of the power spectrum. The following equation describes the power spectral density of the scatter detector current, as described before:

$$P(f) = 4 * I_0 * I_s * (K/\pi) / (f^2 + K^2)$$

This function is maximum at $f = 0$ and drops off at higher frequencies as shown in figure 24. I_s is proportional to the square of the particle diameter for larger particles and to the sixth power of the diameter for smaller particles. K is inversely proportional to the particle diameter. So smaller particles produce more high frequency scatter signal, but with much lower amplitude. Since these low amplitude high frequency signals are mixed with high amplitude low frequency signals, the analog to digital conversion (ADC) bit error noise shows higher percentage errors for the smaller particles. One method to reduce these errors is to use an analog filter before the ADC to attenuate the lower frequency components more than the high frequency components and use either higher optical intensity or electronic gain to increase the signal to fill the range of the ADC. In this way the spectrum of the scatter signal is made more spectrally uniform before digitization. After the signal is digitized and the power spectrum is created, the power spectrum can be divided by the power spectral transmission vs. frequency values for the analog filter to restore the original spectrum of the signal before the filter.

Another method to reduce noise in the scatter signal is to measure self-beating (homodyning) instead of heterodyning. Figure 20 shows a homodyning scatter probe which uses pinholes to define a scatter interaction volume with the source beam. Lens 1 focuses the source beam through a mirror and an optical window with two concave surfaces which have a common center of curvature. The particle dispersion fills the concave surface which is closest to the focus spot or interaction volume. Two scatter detectors collect scattered light through pinholes which view a volume common with the best focus volume of the source. This common volume is called the interaction volume because only particles in this volume can interact with the source beam and produce scattered light at the detectors. Detectors 1 and 2 collect scattered light through pinholes 1 and 2 respectively and lenses 3 and 2 (collector lenses) respectively. These detectors provide dynamic scattering signals from two different scattering angles, which may provide better particle size information. The entire optical assembly could be placed into a probe enclosure which could be inserted directly into the particle dispersion. Also more scattering angles could be measured by adding more collector lens/pinhole/detector assemblies which all view the same volume through the concave surfaces. The possibly expensive double concave surface optic could also be replaced by a standard plano concave lens and a prism as shown in the bottom portion of Figure 20.

This system is designed to measure dynamic light scattering in the homodyne mode, without a local oscillator which usually causes scatter signal noise. Both detectors only see scattering from the interaction volume which could be very close to the inner concave surface, providing very short optical path for scattered rays and reduced multiple scattering at high particle concentrations. This configuration may have advantages when measuring very small particles whose scattering signal is lost in the fluctuations of the

background signal caused by small fluctuations in the large local oscillator needed for heterodyne detection. However, in some cases (larger particles), heterodyne detection is still the optimal detection means. Figure 23 shows how the ideas in Figure 20 can be adapted for heterodyne detection by using fiber optics and fiber optic couplers to distribute and mix source light with the scattered light at each detector. Lens 4 focuses the source light into the fiber optic which guides the light to lens 1 as shown in figure 20. A portion of the light is split off by a fiber coupler 1 and distributed to other couplers, 2 and 4, which mix the source light with the scattered light which is collected by lenses 2 and 3. Scattered light which is collected by lens 2 or lens 3 is guided by two separate fiber optics to scatter detectors 2 or 1, respectively. The source light from fiber coupler 1 is split by fiber coupler 3 to be distributed to fiber couplers 2 and 4 for mixing with scattered light for detectors 2 and 1, respectively. This fiber optic system could also be replaced by the analogous waveguide structures in an integrated optic chip.

Another configuration for using the design, shown in Figure 20, in heterodyne mode is shown in Figure 22. This concept is very similar to that in Figure 20, except that a portion of the source beam is split off by beam splitter 1 to be combined with the scattered light on scatter detector 2 through beam splitter 2. This configuration provides two advantages: the high signal to noise of heterodyne detection and very low back reflection into the light source. Back reflection into laser sources can cause excess laser noise. The back reflections can be further reduced by anti-reflection coating of optical surfaces, in particular, the first air-glass surface of the concave optic. Figure 22 shows the combination of a heterodyne channel (detector 2) and a homodyne channel (detector 1). However, the source light transmitted through beam splitter 2 could also be combined with the detector 1 scattered light using a third beam splitter to produce a second heterodyne channel. Figure 21 shows a method for creating the concave optic from two or three mass produced optics. A plano-convex lens and plano-concave lens are positioned so that the centers of curvature for their curved surfaces are coincident at the interaction volume. If required, a plano spacer can be placed between these two optics. In any case, all plano surfaces can be bonded to the adjacent plano surface with index matching adhesive to reduce internal reflections.

One source of signal noise in fiber optic dynamic light scattering systems is interferometric noise due to motion of the optical fibers. This noise can occur in both single and multimode fiber optics and couplers. Figures 25 and 26 show two concepts for reducing the fiber motion by potting the fiber optic assembly in a solid potting material, which can be cured from a liquid to a solid. Most potting materials will work well, but materials with high thermal conductivity and/or low thermal coefficient of expansion may be most appropriate. Figure 25 shows the fiber optic system, from Figure 19, potted with fiber optic connectors to the light source and detectors which remain outside of the potted volume (but one half of each connector is potted into the potted volume). This provides for replacement of the detector or light source. Figure 26 shows the same fiber optic system which is entirely potted, with access to the detectors and light source through electrical connections needed for powering and monitoring the source and detector. The detector at port three can also be outside of the potted volume and connected by a fiber optic connector to port 3 (as shown in Figure 25 for port 2) or it

could be potted into the structure and accessed through an electrical conduit as shown in Figure 26 for port 2. In Figure 26, the optical path must be kept free of potting material to avoid attenuation or distortion of the optical beam. These voids in the potting volume are not explicitly shown in Figure 26. Depending upon the mechanism creating the interferometric noise, the fiber optic cable sheath and/or fiber optic buffer could be removed so that the potting material adheres directly to either the buffer or the cladding of the fiber. Or In cases where only the cable needs to be immobilized and the fiber can be allowed to move within the cable, the cable can be left on the fiber. Then the potting material will adhere to the cable surface. In any case, this potting method should reduce the frequency and amplitude of the fiber motion induced noise so that it can be removed from scatter signal as a small correction.

Figure 27 shows another version of the fiber optic system, where the source light is mixed with the scattered light through fiber optic port 3. In this case, the surfaces in the scatter collection optics, at port 4, are anti-reflection coated to avoid back reflections of source light into port 2. This provides two advantages. Firstly, the amount of light out of port 3 can be much larger than the light that was intentionally back reflected from port 4, in Figure 10, creating a larger local oscillator. Additionally, very little light is back reflected into the light source in this design. Back reflection into laser sources can cause excess laser noise. In all of the cases shown in this disclosure, back reflection into light source can be reduced by use of a polarizer and quarter wave plate to produce an optical isolator at the exit of the light source assembly. However, this requires the use of expensive single mode polarization preserving fiber optics and couplers; and it produces circular polarized light at the particles. And it will also not work with multimode fiber optics. However, this disclosure claims the use of an isolator to reduce back reflections into the laser to reduce laser amplitude and phase noise in this application, when it is appropriate.

In some cases, very large particles can contribute scatter signals which will distort the signals from smaller particles. In this case, particle settling could be used to remove larger particles from the interaction volume, as shown in Figure 28 which shows a variation on the concept in Figure 9. The sample chamber has an extension above the interaction volume so that particles cannot settle into the interaction volume from above. Hence, the interaction volume will gradually be depleted of larger particles, which settle out of the volume. Scatter data can be collected at various times during this settling process to measure different size ranges of the distribution separately. This concept is also described in more detail in another disclosure by this inventor. The bottom portion of the sample cell enclosure is shortened or removed completely to allow the particle dispersion to flow down and out of the interaction volume when the sample cell is emptied and rinsed in preparation for the next sample.

As mentioned before, one cause of laser noise is laser light which is reflected back into the laser. Figures 29 and 30 show versions of Figures 4 and 8, respectively, where a polarizing beamsplitter and quarter wave plate are utilized to increase the optical efficiency of the detection path and reduce the light back-reflected into the laser. The polarizing beam splitter is oriented to provide maximum transmission for the polarization

of the laser. The polarized light passes through a quarter wave plate with axes at 45 degrees to the polarization direction of the source. The local oscillator light, which is reflected back from the convex surface in Figure 29 or from the partial reflecting mirror in Figure 30, will pass back through the quarter wave plate on the return path towards the polarizing beamsplitter. In both cases, the light gains a second quarter wave of phase in one polarization, accumulating a total of one half wave which will rotate the polarization by 90 degrees. When passing back through the polarizing beamsplitter, the 90 degree polarization rotated light will be reflected by the beamsplitter and very little light will transmit through the beamsplitter to be focused back into the laser source. The scattered light will propagate through the same process, and also be reflected by the polarizing beamsplitter. So both the source light and scattered light will be reflected by the polarizing beamsplitter through the lens 4 to the detector, where mixing, of the local oscillator and scattered light, and heterodyne detection of the scattered light occurs. Any flat surfaces between lenses 2 and 3, except for a surface which reflects the local oscillator, shall be tilted slightly so that the reflection from that surface will not pass into the laser source. For example, the beamsplitter and quarter wave plate should both be tilted slightly off of normal to the optical axis so that reflections from their surfaces cannot pass back to the laser. All of these surfaces, except for those reflecting the local oscillator reflection, should also be anti-reflection coated. The end of a polarization preserving fiber optic with attached scattering optic assemblies, as shown previously in this disclosure, could also be aligned with the final focal point (in the interaction volume) of either Figure 29 or Figure 30 to provide a flexible extension and scattering probe. In this case, the local oscillator could be created by a reflecting surface inside of the scattering optics assembly so that the scattered light and local oscillator travel through the same optical paths to get to the detector.

Other Noise Correction Techniques

The basic fiber optic interferometer is illustrated in Figure 10. A light source is focused into port 1 of a fiber optic coupler. This source light is transferred to port 4 and light scattering optics which focus the light into the particle dispersion and collect light scattered from the particles. This scattered light is transferred back through the fiber optic and coupler to the detector on port 2. If the coupler has a third port, a portion of the source light also continues on to port 3 which may provide a local oscillator with a reflective layer. If the local oscillator is not provided at port 3, a beam dump or anti-reflective layer may be placed onto port 3 to eliminate the reflection which may produce interferometric noise in the fiber optic interferometer. The beam dump could consist of a thick window which is attached to the tip of the fiber with transparent adhesive whose refractive index nearly matches that of the fiber and the window. This will reduce the amount of light which is Fresnel reflected back into the fiber at the fiber tip. The other surface of the window can be anti-reflection coated, and/or be sufficiently far (thick window) from the fiber tip, to minimize the reflected light, from that surface, that can enter the fiber.

Figure 11A shows one version of the scatter optics on port 4. A lens or gradient index optic (GRIN) focuses the source light into the particle dispersion in a cuvette through a transparent wall of the cuvette. A partially-reflective layer on the tip of the fiber or on the surface of the GRIN rod, at the fiber/GRIN gap, provides the local oscillator light to travel back through port 4 with light scattered by the particles. If the fiber surface is partially reflecting, the GRIN surface could be anti-reflection coated or it could be placed sufficiently far from the fiber to avoid reflections from the GRIN surface back into the fiber. Reflections from both surfaces could produce an optical interference signal which may contaminate the heterodyning signal from the scattering particles. The reflected source light and the scattered light, from particles in the cuvette, travel back through the coupler and are combined on the detector at port 2. The interference between these two light components is indicative of the Brownian motion of the particles and the particle size. Since the local oscillator is generated at the exit surface of port 3 or port 4, as opposed to the cuvette surface, the interference signal is not degraded by small errors in the position of the cuvette surfaces, allowing use of inexpensive disposable cuvettes. The local oscillator is provided by light reflected from either port 3 or port 4 fiber optic.

Other designs for port 4 could incorporate a window, on the surface of the GRIN rod, which contacts the particle dispersion directly. The details of other designs have been disclosed by this inventor in other disclosures.

The port 2 detector current is digitized for analysis to determine the particle size in the dispersion. The power spectrum of the optical detector current contains a constant local oscillator and a frequency dependent component. The frequency dependent component is described by the following equations:

$$P(f) = (S(d,a,n)^2) * (D * K^2) / (4\pi^2 * (f)^2 + (DK^2)^2) + n(f)$$

where $K = 2 * n * \sin(a/2) / \lambda$

$$D = kT / (3 * \pi * \eta * d)$$

$P(f)$ = power spectral density of the detector current (or voltage) at frequency f

S = scattering efficiency per unit particle volume

d = particle diameter

η = dispersant viscosity

f = frequency

n_p = refractive index of particle

n_m = refractive index of dispersant

a = scattering angle

c = constant which depends on dispersant viscosity and particle shape

\wedge^2 = square of quantity

g = acceleration

k = Boltzman's constant

T = dispersant temperature

λ = wavelength of the source light

$n(f)$ = baseline noise power spectral density

This equation describes the power spectrum from a single particle of diameter d . For groups of particles of various sizes, the power spectrum is the sum of the spectra from the individual particles. Then the total spectrum must be deconvolved to find the particle size distribution. Usually the spectrum from clean dispersant is measured to determine $n(f)$, which is the portion of the spectrum due to laser noise, detector noise, modal interference due to fiber optic vibrations, and other noise sources. This baseline noise is the power spectrum measured without any particles in the dispersant. This baseline noise spectrum is subtracted from the power spectrum measured from the particles to determine the spectrum which is only due to Brownian motion of the particles. However, $n(f)$ is not usually stable during the period required to gather sufficient digitized data to create an accurate estimation of the power spectrum.

One useful property of the fluctuating portion of the baseline noise is that the noise is nearly white and shows strong correlation with values of $n(f)$ at high frequencies. As shown by the equation for $P(f)$, the power spectrum component due to light scattered from the particles drops off very rapidly at high frequencies and becomes negligible as compared to $n(f)$ at high frequencies. At high frequencies, the particle scatter portion of the spectrum drops as $1/f^2$. In any event the detector current could be sampled at sufficiently high frequencies to measure the power spectrum where the contribution from the particles is small.

One method for noise correction is to generate an empirical set of $n(f)$'s by measuring $n(fp)$ in the frequency region where the particles contribute to $P(f)$ while also measuring $n(fh)$ at high frequencies where the particle contribution would normally be small. So various $P(f)$'s are measured without particles to generate a function G :

$$n(fp) = G(n(fh))$$

The portion of the spectrum $n(fh)$ could be measured from the calculated power spectrum of the digitized data. But then the detector current must be sampled at rates well beyond those required to measure the particles. The value for $n(fh)$ could also be measured by band pass analog filters and power circuits, to generate the total power in a bandpass in frequency regions which capture frequencies where the particles will have very small contributions.

In either case, once the function $G(n(fh))$ is created, it can be used to correct the spectrum measured from particles by measuring $n(fh)$ each time an FFT is created to produce a contribution to the total power spectrum of the entire measurement period. This particular $ni(fp) = G(ni(fh))$ is then subtracted from the $Pi(f)$ for the i th data segment to correct that data segment for the $n(f)$ during that segment. In this way, as $ni(f)$ fluctuates, the i th segment is corrected precisely for its noise. This could also be accomplished by summing all of the $Pi(f)$'s over i to get $Pt(f)$ and all of the $ni(f)$'s over i to get $nt(f)$ and then using $Pt(f) - nt(f)$ to calculate the spectrum contribution from the particles.

$G(n(f))$ could also be determined from data points in both the upper f_p and f_h regions to produce better conditioning of the simultaneous equations used to solve for the parameters in the function G . In any case, if the fluctuating component of $n(t)$ is white noise and is flat out to f_h , then the correction is simple because $n(f_p) = n(f_h)$. But in general, a function G may be required to get precise correction over the entire range of fluctuations. G can take the form of a polynomial function of f (over both regions f_p and f_h) or a group of $n(f_p)$ functions in a look-up table, where interpolation between the 2 table $n(f_p)$ functions, with the closest corresponding values for $n(f_h)$ to the measured value of $n(f_h)$, would be used to determine the $n_i(f_p)$ for the i th data segment. In some cases, G will be proportional to the inverse of the square-root of frequency f .

This correction procedure is only required in the frequency regions where the fluctuations in $n(f)$ cause unacceptable errors in the calculated particle size distribution. Typically this will be in the higher frequency end of the f_p region, where the smaller particle information is contained. At lower frequencies, a single measurement of $n(f)$ before or after the particle measurement may be sufficient, without using G .

Another method which may be utilized is to solve entire the problem in a generalized fashion. This method would use all of the power spectrum data, $P(f_p)$ and $P(f_h)$, to solve for the particle contribution and baseline contribution using an iterative procedure which assumes the existence of both. However, the G function method described above may be more effective because more a priori knowledge is provided to the algorithm.

These methods can be applied to the power spectrum on any frequency scale, including but not limited to a logarithmic progression in f . However, if the fluctuating portion of the baseline noise is nearly white or uniform in density, then a linear scale in f may be optimal for calculation of G .

The background can be solved for as part of the total solution in this background drift problem and many other similar problems where a system model is inverted to solve for the particle size distribution. Consider the generalized model below:

$$F = H * V$$

Where F is the measured data (power spectrum of scattered light signal, angular distribution of scattered light, etc.), V is the size distribution to be solved for, and H is the matrix which describes the system model (Brownian motion/Doppler effect, angular light scattering, etc.). This model is usually inverted to produce the size distribution:

$$V = F/H$$

Where F/H represents the solution of the matrix equation by any means including iterative techniques with constraints on the values of V . The actual values for F are calculated by subtraction of the actual background from the measured F , which includes the background.

$$FB_{\text{measured}} = F_{\text{actual}} + B_{\text{actual}}$$

Inventor: Michael Trainer

Where F and B are the actual scattering data and the background (without particles), respectively

However the computed values (called Fc) for F use the measured values of B which may differ from the actual values of B (due to drift of B) by the error vector E.

$$B_actual = B_measured + E$$

$$F_c = FB_measured - B_measured$$

$$F_c = F_actual + E$$

Then the matrix equation above becomes:

$$F_c - E = H*V$$

Solving this matrix equation for V, we obtain

$$V = (F_c - E)/H \quad (/ \text{ is not a literal division, } / \text{ represents solution of the matrix equation above for } V)$$

If V has m unknowns, F has n measured values, and E is described by k number of parameters, then V and E can be solved from this equation as long as $m + k \leq n$. This method works well when E is much smaller than B_measured so that the correction E is small and accurately described using only a few parameters. For example, in the previous case, E could be simply white noise times a constant which determines the amount of white noise which must be added to the noise background, which was measured without particles in the source beam, in order to obtain the best result for V, or in other words the result which minimizes the RMS error:

$$SQRT((F_c - E)^2 + (H*V)^2)$$

This function can be minimized by known iterative methods, such as simply changing E and inverting $F_c - E = H*V$ multiple times and choosing the result for V and E which minimizes the RMS error above.

Particle detection

Semiconductor processes require very clean fluids with less than one 0.1 micron particle per cubic meter. The light scattered by a particle of this size can be detected as it passes through a focused laser beam. However at 10 meters per second flow rate, interrogation of a cubic meter of fluid would consume over 3 years through a laser volume of 1000 cubic microns (cubic volume of 10 microns on each side). This invention describes an apparatus for detecting the presence of one particle per cubic meter at a rate of 1 cubic meter per hour. The system is shown in Figure 31.

A light source is projected into a sample flow tube by lens 1. The optics may be adjusted to collimate the beam within the tube or to produce a beam waist inside the tube. Beam splitter 1 reflects a portion of the beam onto lens 2 which focuses that light onto detector 2. Detector 2 measures the source intensity to correct for source fluctuations. The unreflected portion of the beam proceeds through beamsplitter 2 which reflects a portion of the beam back through lens 3, providing a local oscillator for heterodyne detection of scattered light from particles in the sample flow tube. The unreflected portion of the beam proceeds through optical window 1 and travels down a long sample tube, through which the test fluid is pumped. Window 2 allows the beam to exit the tube with minimal reflections back into the tube. Any particle passing down the tube will scatter light back to detector 1 through beam splitter 1, lens 3 and a pinhole which maintains coherence requirements for heterodyne detection and eliminates background light from hitting detector 1.

The major advantage of this system is the large crosssection of the interrogated volume in the sample flow tube and the long interaction distance within the tube, which could be meters in length. The two detector currents, I1 from detector 1 and I2 from detector 2 can be described by the following equations:

$$I1 = \sqrt{R \cdot I_o(t) \cdot I_s(t)} \cdot \cos(F \cdot t + A) + R \cdot I_o$$

$$I2 = K \cdot I_o(t)$$

where:

$\cos(x)$ = cosine of x

K is a constant which includes reflectivity of beam splitter 1

R is the reflectivity of beamsplitter 2

\sqrt{x} = square root of x

$I_o(t)$ is the source beam intensity as function of time t

F is the heterodyne beat frequency at detector 1 due to the motion of the scatterer in the flow tube. And A is an arbitrary phase angle for the particular particle.

$I_s(t)$ is the scattered light intensity from the particle:

$I_s(t) = S \cdot I_o(t)$ where S is the scattering efficiency or scattering crosssection for the particle

The light source intensity will consist of a constant portion I_{oc} and noise $n(t)$:

$$I_o(t) = I_{oc} + n(t)$$

We may then rewrite equations for I1 and I2:

$$I1 = \sqrt{S \cdot R} \cdot (I_{oc} + n(t)) \cdot \cos(F \cdot t + A) + R \cdot (I_{oc} + n(t))$$

$$I2 = K \cdot (I_{oc} + n(t))$$

The heterodyne beat from a particle traveling with nearly constant velocity down the flow tube will cover a very narrow spectral range with high frequency F. For example, at 1 meter per second flow rate, the beat frequency would be in the megahertz range. If we use narrow band filters to only accept the narrow range of beat frequencies we obtain the narrow band components for I1 and I2:

$$I1_{nb} = \sqrt{S \cdot R} \cdot I_{oc} \cdot \cos(F \cdot t + A) + R \cdot n(t)$$

$$I2_{nb} = K \cdot n(t)$$

where we have assumed that $n(t)$ is much smaller than I_{oc} .

The laser noise can be removed through the following relationship:

$$\sqrt{S} \cdot I_{oc} \cdot \cos(F \cdot t + A) = I1_{nb} - (R/K) \cdot I2_{nb}$$

This relationship is realized by narrowband filtering of each of the I1 and I2 detector currents. One or both of these filtered signals are amplified by programmable amplifiers, whose gains are adjustable. The difference of the two outputs of these amplifiers is generated by a difference circuit or differential amplifier. With no particles in the beam, the gain of at least one of the programmable amplifiers is adjusted, under computer control, to minimize the output of the difference circuit. At this gain, the source intensity noise component in the detector 1 beat signal is corrected for in the difference signal, which is fed to an analog to digital converter (A/D), through a third narrowband filter, for analysis to sense the beat signal buried in noise. This filtered difference signal could also be detected by a phase locked loop, which would lock in on the beat frequency of current from detector 1.

This entire correction could be accomplished in the computer by using a separate A/D for each filtered signal and doing the difference by digital computation inside the computer. If both signals were digitized separately, other correlation techniques could be used to reduce the effects of source intensity noise. The real advantage of this measurement is the high frequency beat signal is produced for the duration of the particle's residence in the long flow tube. This could produce millions of beat cycles during the particle's transit, allowing phase sensitive detection in a very narrow bandwidth at megahertz frequencies, well above any 1/f noise sources. The power spectrum of a data set consisting of a large number of signal cycles will have a very narrow spectral width, which can be discriminated against broad band noise, by using the computed power spectrum of the signal and spectral discrimination algorithms. Beamsplitter 2 reflection is adjusted to

Inventor: Michael Trainer

obtain shot noise limited heterodyne detection, with excess laser noise removed by the difference circuit.

This Page Is Inserted by IFW Operations
and is not a part of the Official Record

BEST AVAILABLE IMAGES

Defective images within this document are accurate representations of the original documents submitted by the applicant.

Defects in the images may include (but are not limited to):

- BLACK BORDERS
- TEXT CUT OFF AT TOP, BOTTOM OR SIDES
- FADED TEXT
- ILLEGIBLE TEXT
- SKEWED/SLANTED IMAGES
- COLORED PHOTOS
- BLACK OR VERY BLACK AND WHITE DARK PHOTOS
- GRAY SCALE DOCUMENTS

IMAGES ARE BEST AVAILABLE COPY.

**As rescanning documents *will not* correct images,
please do not report the images to the
Image Problem Mailbox.**

Figure 1

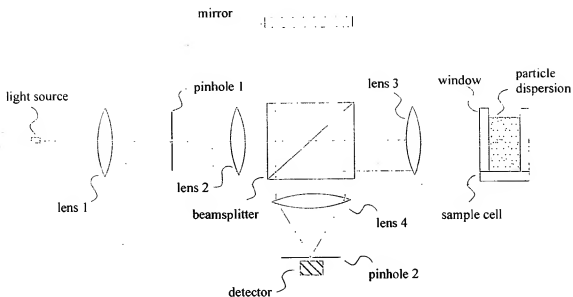


Figure 2

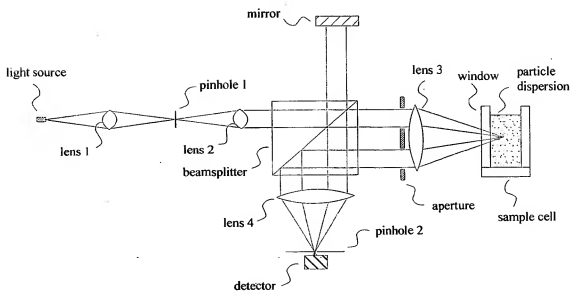


Figure 3

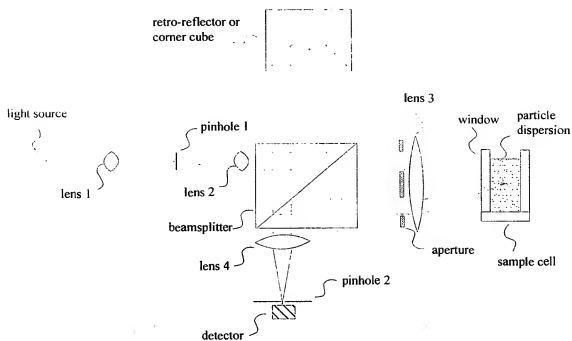


Figure 4

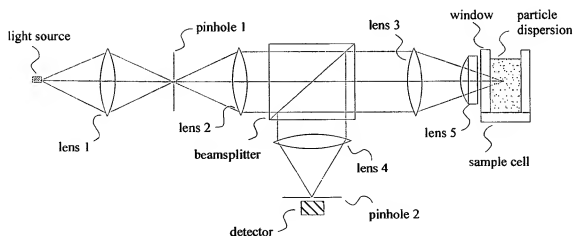


Figure 5

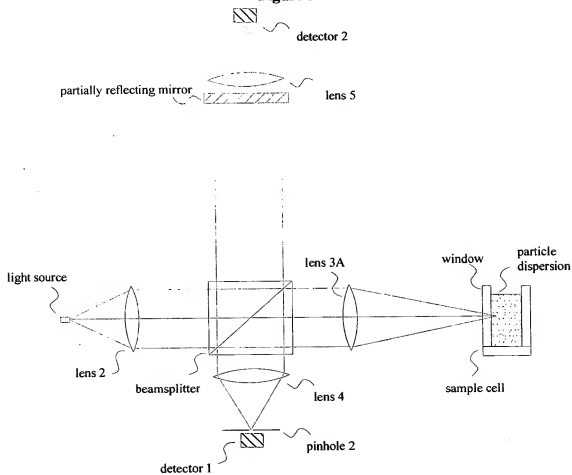


Figure 6

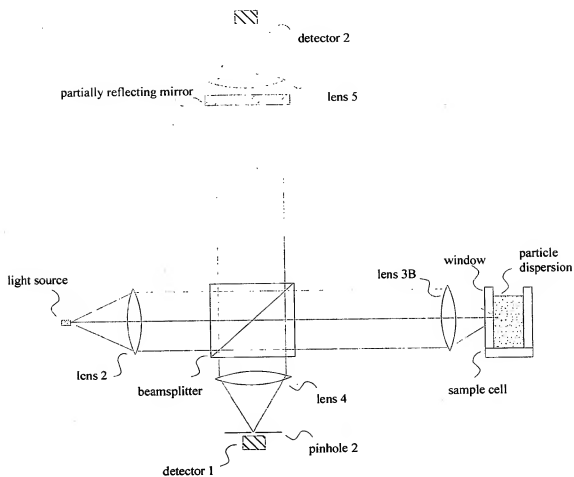


Figure 7

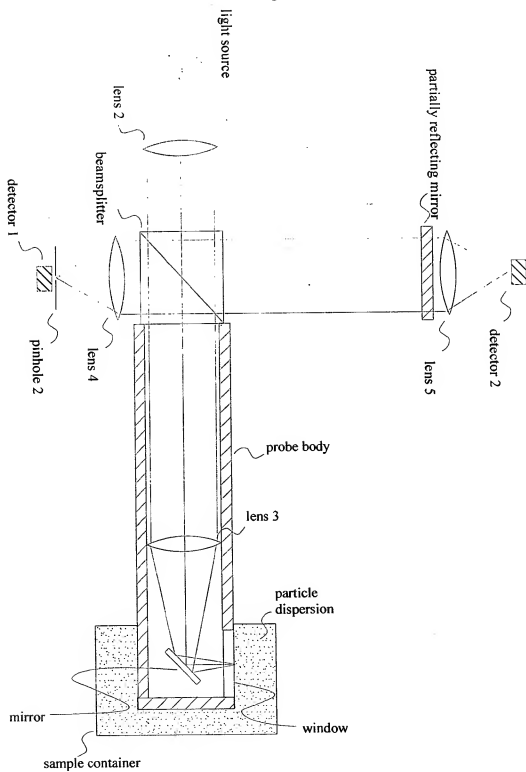


Figure 8

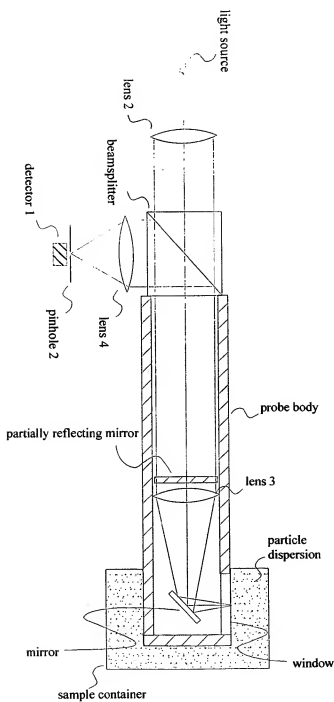


Figure 9

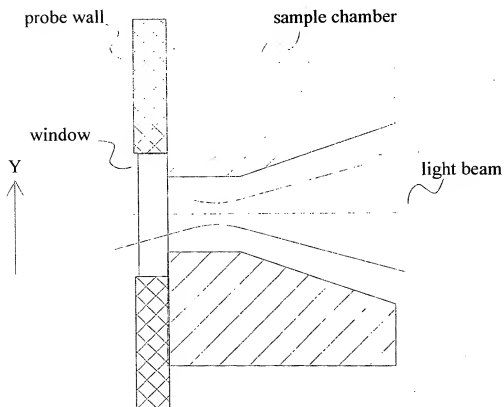


Figure 10

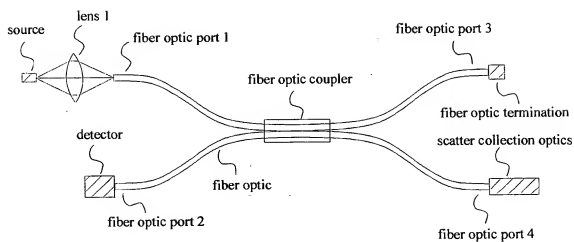


Figure 11A

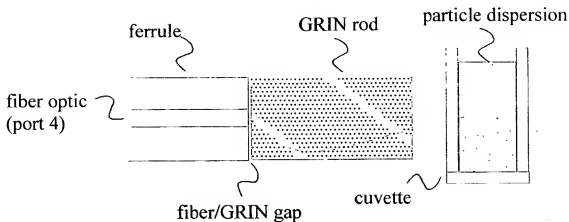


Figure 11B

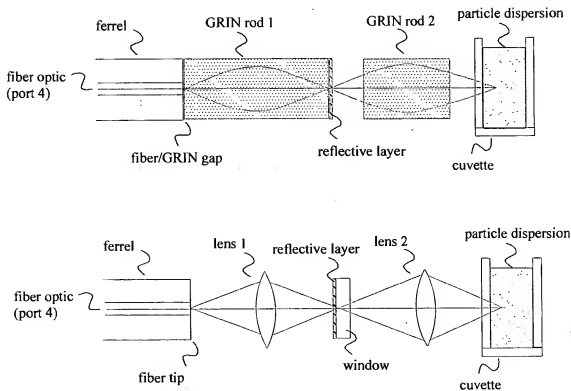


Figure 12

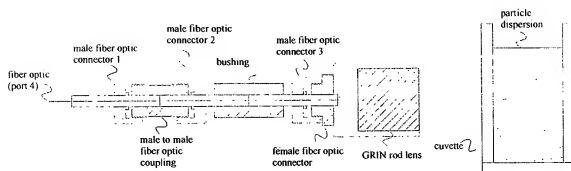


Figure 13

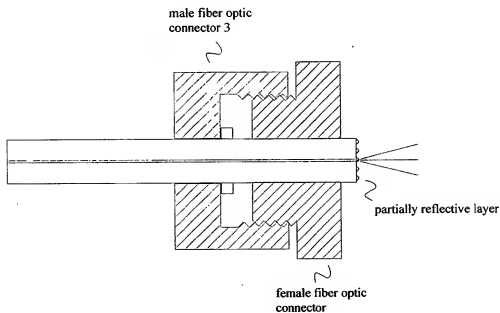


Figure 14

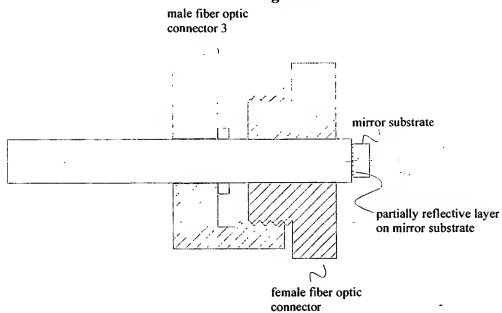


Figure 15

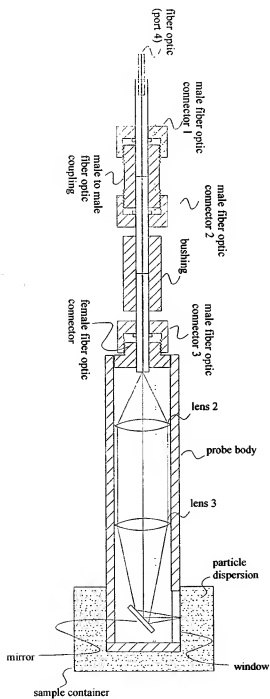


Figure 16

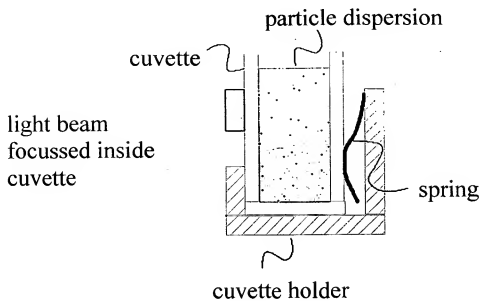


Figure 17

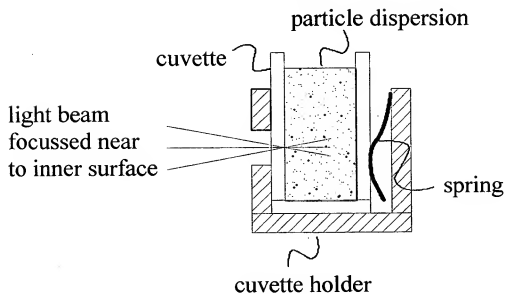


Figure 18

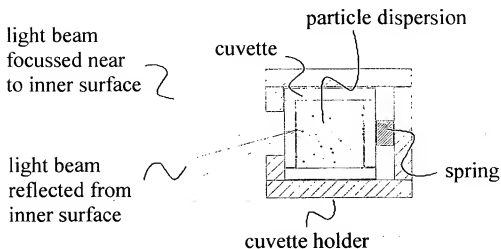


Figure 19

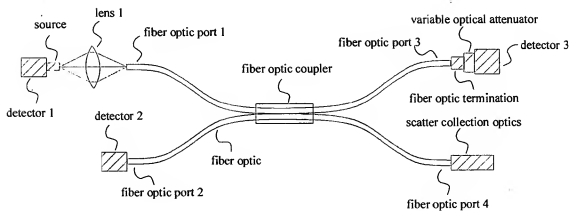


Figure 20

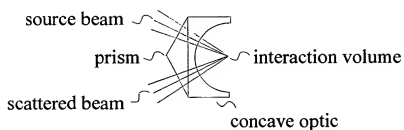
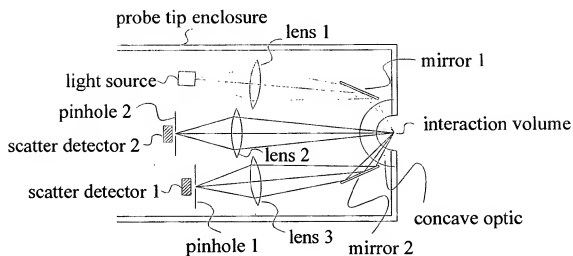


Figure 21

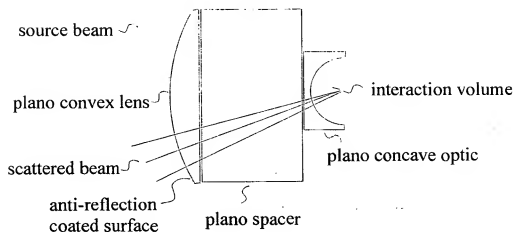


Figure 22

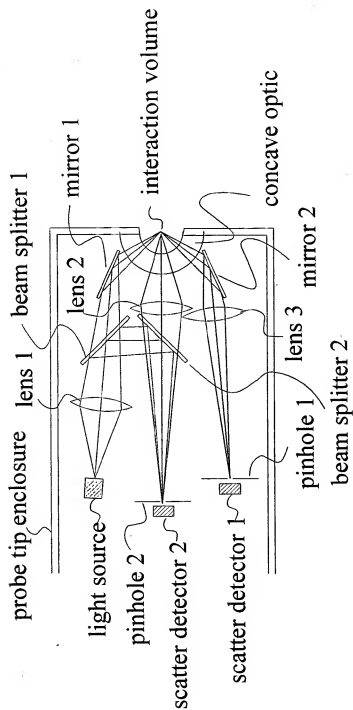


Figure 23

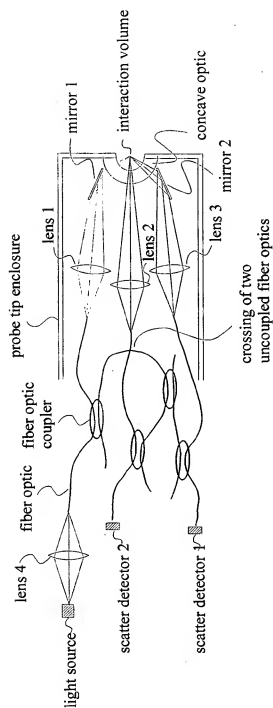


Figure 24

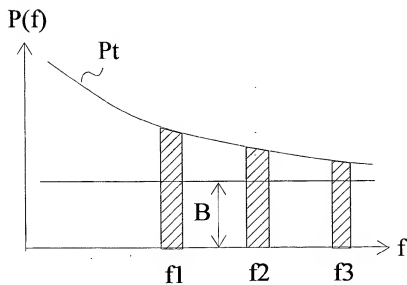
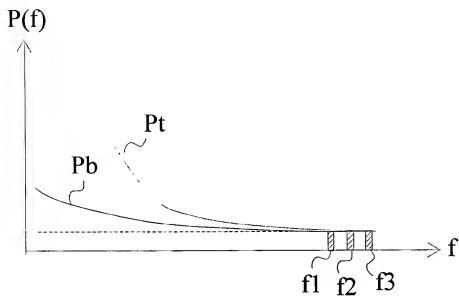


Figure 25

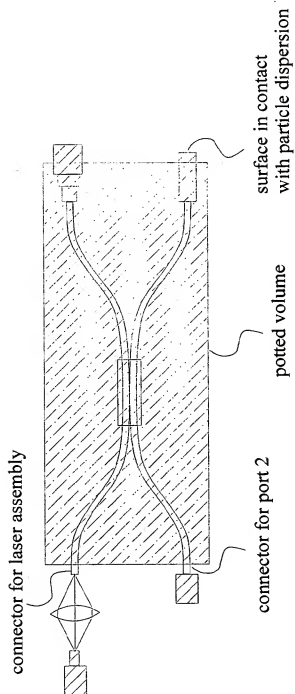


Figure 26

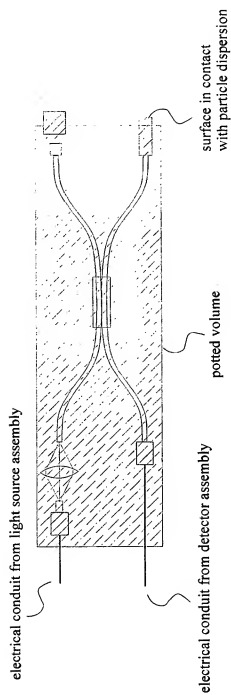


Figure 27

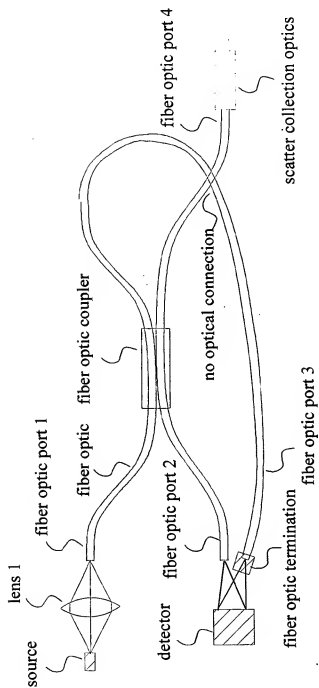


Figure 28

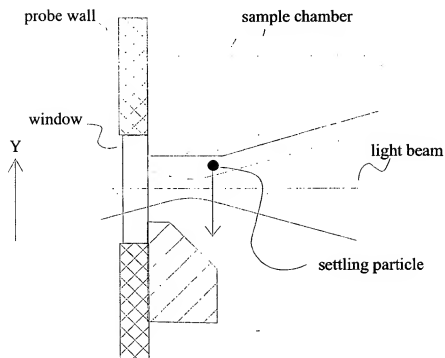


Figure 29

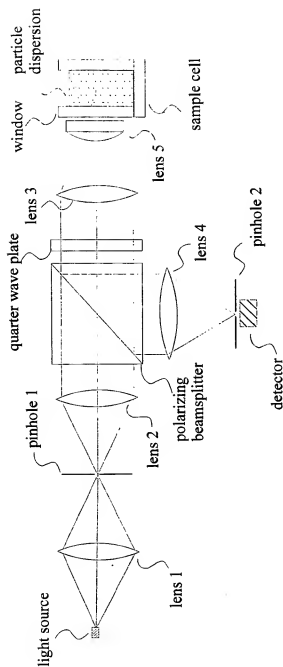


Figure 30

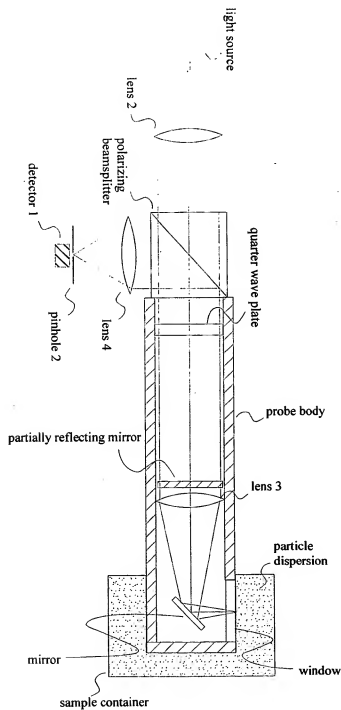


Figure 31

